

## Effective conductivity of UO<sub>2</sub>

Bohyun Yoon<sup>a</sup>, Kunok Chang<sup>a\*</sup>

<sup>a</sup>Department of Nuclear Engineering, Kyung Hee University, Yong-in, Korea

\*Corresponding author: kunok.chang@khu.ac.kr

### 1. Introduction

The irradiated UO<sub>2</sub> pellets contains defects, such as grain boundaries, voids and fission gas bubbles. These microstructural inhomogeneities affect the thermal conducting properties of nuclear fuel. There have been studies to predict the effective conductivity of porous nuclear fuel. However, the effect of pore radius has not been thoroughly examined in those studies [1-4]. We performed steady-state heat conduction analyses of the given systems of UO<sub>2</sub> and analyzed the effect of said factor on the conductivity.

### 2. Physical model description

#### 2.1 Microstructure and temperature dependence on the local conductivity

We introduced the structural order parameter  $\eta(r)$  to make local conductivity depend on the microstructure. Its value is 0 in the He bubbles, 1 at the matrix and lower than 1 in the grain boundary region. The thermal conductivity of Helium gas is fixed at 0.152 W/(K·m). We adopted the model suggested by Harding and Martin for the conductivity of UO<sub>2</sub> crystal which has the following temperature dependence in the unit of W/(K·m) [5].

$$k_{crystal} = \frac{1}{0.0375 + 2.165 \times 10^{-4} T} + \frac{4.715 \times 10^9}{T^2} \exp\left(\frac{-16361}{T}\right) \quad \dots (1)$$

The structural order parameter  $\eta(r)$  has following effect on the local heat conductivity. Thus thermal conductivity is lower in the grain boundary than it is in the matrix region.

$$k(r) = \sum_i \eta_i^{7.7}(r) \times k_{crystal} \quad \dots (2)$$

Miller et al. proposed effective conductivity model of polycrystalline UO<sub>2</sub> with pores as follows [6]:

$$k_{eff} = \frac{k_0}{1 + k_0/G_k d} (1 - P)^\beta \Psi \quad \dots (3)$$

where  $G_k$  is a Kapitza conductance,  $d$  is an average grain diameter,  $\beta$  is a fitting parameter and  $\Psi=1-P$  is a correlation factor that relates 2-D to 3-D heat transport in porous media.

In Eq. 4, which is ‘‘Schulz equation’’ [7],  $\beta$  is determined by geometry of pores.

$$k_{eff} = k_0 (1 - P)^\beta \quad \dots (4)$$

Nikolopoulos and Ondracek predicted  $\beta=2.5$  for spherical pores and  $\beta=1.667$  for cylindrical pores which statistically directed to the field direction in isotropic materials. [8]

#### 2.2 Steady-state thermal conduction analysis

We solved steady-state heat conduction equation:

$$\nabla k(r) \nabla T(r) = 0 \quad \dots (5)$$

We simulated 20.48  $\mu\text{m}$  ( $L_x$ )  $\times$  20.48  $\mu\text{m}$  ( $L_y$ ) two-dimensional system. The simulation cell size is 2048 $\times$ 2048 grid points, therefore  $\Delta x = \Delta y = 10$  nm. Dirichlet boundary condition of  $T=800\text{K}$  is applied on the left side of the system. Neumann boundary condition of  $j = k(r) \frac{\partial T(r)}{\partial x} = 50\text{MW/m}^2$  is applied across the right side. We applied the adiabatic condition,  $\frac{\partial T(r)}{\partial x} = 0$  on top and bottom. The simulation cell is depicted in Fig. 1. The effective thermal conductivity is evaluated by the relation [9]:

$$k_{eff} = \frac{j \times L_x}{\Delta T} \quad \dots (6)$$

where  $j$  is the heat flux and  $\Delta T$  is temperature drop across the system.

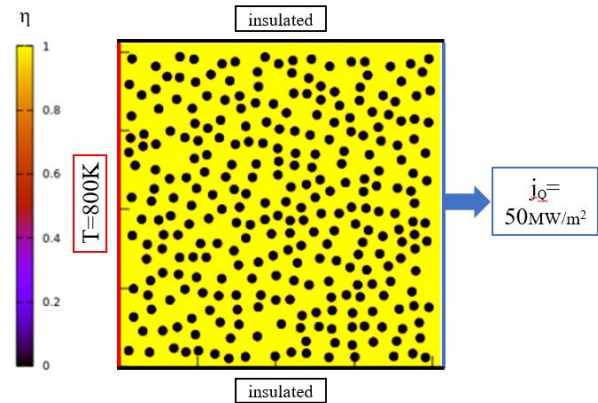


Fig. 1. Microstructure with porosity=19%, pore diameter=20 nm.

#### 2.3 Crank-Nicolson method

The steady-state heat conduction equation was solved using a finite-difference approximation with a Crank-Nicolson scheme (CN) and alternating-direction-implicit (ADI) method. The CN scheme is an implicit method which discretizes time and space. And we apply Douglas-Gunn’s ADI splitting method [10] to decompose the discretization matrix of the CN scheme. This ADI method splits the matrix into three simple matrices introducing intermediate time steps between  $n$  and  $n+1$ .

We used parallel computing method to accelerate the computation speed. It made time required for the

calculation approximately 10% of that using a serial code.

### 2.4 Porous material with different pore radii

To examine the pore size effect on effective conductivity, we measured effective conductivity with different pore sizes. The typical microstructure used in the simulation and its temperature distribution are given in Fig. 2. We found that the exponent  $\beta$  in Eq. 4 increases as the pore size decreases, which means small pore-sized structure has stronger dependency of porosity in effective conductivity rather than large pore-sized structure.

### 3. Conclusions

In this work, we have investigated a role of pore size on the effective conductivity of  $\text{UO}_2$  using a computational method at the continuum-level. The calculations indicate that small pores are more effective in reducing effective conductivity rather than large pores at given. We fitted the exponent value  $\beta$  of Schulz equation as shown in Fig. 3 and found that there is a dependence of pore size on exponent  $\beta$  value. We found that  $\beta$  exponent decreases as the pore size increases. And effective conductivity increases as the grain size increases as shown in Fig. 4. We are measuring the effect of grain size on the effective conductivity to establish the thermal conductivity model for the porous  $\text{UO}_2$  polycrystal.

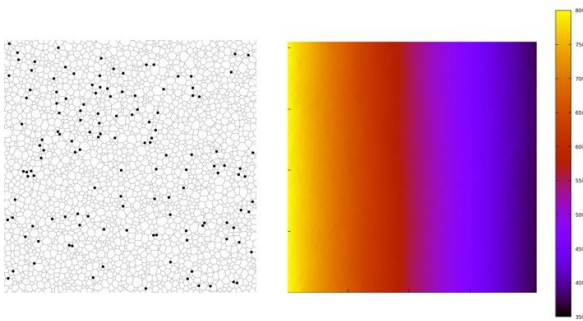


Fig. 2. (left) Microstructure with porosity=1%, average grain diameter=0.4 um. (right) Its temperature distribution at the steady-state in units of K.

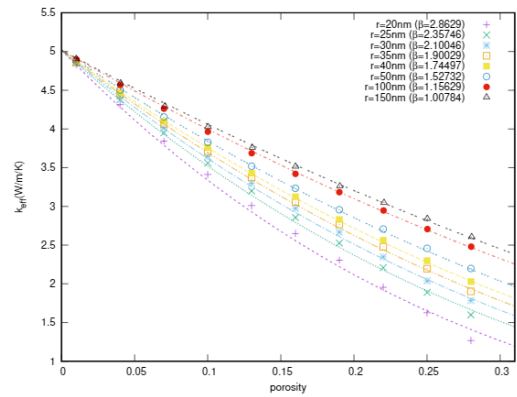


Fig. 3. Effective conductivity as a function of the porosity for different circular pore radii.

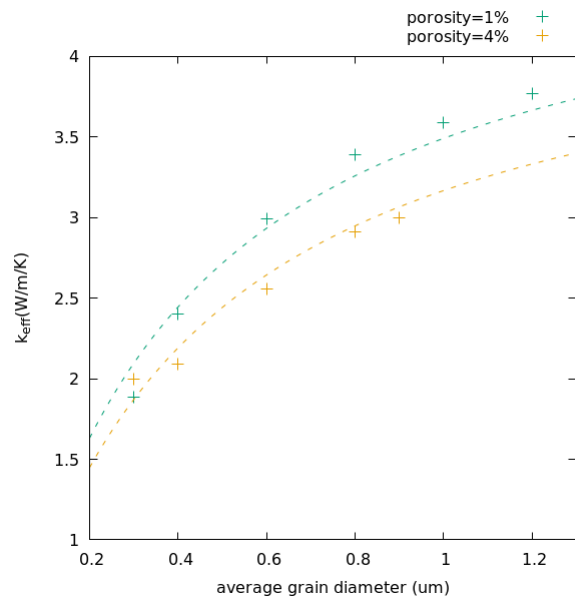


Fig. 4. Effective conductivity as a function of average grain diameter for different porosity.

### REFERENCES

- [1] S. R. Phillpot, A. El-Azab, A. Chernatynskiy, J. S. Tulenko, Thermal conductivity of  $\text{UO}_2$  fuel: Predicting fuel performance from simulation, *Jom* 63 (8), 73, 2011.
- [2] C.-W. Lee, A. Chernatynskiy, P. Shukla, R. E. Stoller, S. B. Sinnott, S. R. Phillpot, Effect of pores and he bubbles on the thermal transport properties of  $\text{UO}_2$  by molecular dynamics simulation, *Journal of Nuclear Materials* 456, 253–259, 2015.
- [3] X.-M. Bai, M. R. Tonks, Y. Zhang, J. D. Hales, Multiscale modeling of thermal conductivity of high burnup structures in  $\text{UO}_2$  fuels, *Journal of Nuclear Materials* 470, 208–215, 2016.
- [4] M. R. Tonks, X.-Y. Liu, D. Andersson, D. Perez, A. Chernatynskiy, G. Pastore, C. R. Stanek, R. Williamson, Development of a multiscale thermal conductivity model for fission gas in  $\text{UO}_2$ , *Journal of Nuclear Materials* 469, 89–98, 2016.
- [5] J. Harding, D. Martin, A recommendation for the thermal conductivity of  $\text{UO}_2$ , *Journal of nuclear materials* 166 (3), 223–226, 1989.
- [6] P. C. Millett, D. Wolf, T. Desai, S. Rokkam, A. El-Azab, Phase-field simulation of thermal conductivity in porous

polycrystalline microstructures, *Journal of Applied Physics* 104 (3), 033512, 2008.

[7] B. Schulz, Thermal conductivity of porous and highly porous materials, *High Temperatures-High Pressures* 13 (6), 649–660, 1981.

[8] P. Nikolopoulos, G. Ondracek, Conductivity bounds for porous nuclear fuels, *Journal of Nuclear Materials* 114 (2-3), 231–233, 1983.

[9] P. C. Millett, M. R. Tonks, K. Chockalingam, Y. Zhang, S. Biner, Three-dimensional calculations of the effective kapitza resistance of  $UO_2$  grain boundaries containing intergranular bubbles, *Journal of Nuclear Materials* 439 (1-3), 117–122, 2013.

[10] J. Douglas, Alternating direction methods for three space variables, *Numerische Mathematik* 4, 41–63, 1962.